Dose Optimization and Reduction in Musculoskeletal CT Including the Spine

A. Gervaise, P. Teixeira, N. Villani, S. Lecocq, M. Louis, and A. Blum

Contents

Abstract

Due to improvements in temporal and spatial resolution, and despite its radiating character, CT is still indicated for the assessment of many musculoskeletal disorders. New exploration techniques, such as dynamic CT of the joints and bone perfusion imaging, are now available in musculoskeletal imaging. However, they require the repetition of many phases and lead to an increase in dose. For these new applications and for spine and proximal joint imaging in the vicinity of radiosensitive organs, optimization and dose reduction are critical. In this chapter, we report the typical doses delivered in musculoskeletal CT examinations and discuss several options for allowing dose optimization and reduction, depending on behavioral and technical factors. Among them, tube current and tube potential optimization are still critical and must be adapted to the type of exploration and the body habitus of each patient. Recent technical factors can also help to reduce the doses such as automatic tube current modulation, active collimation or new CT iterative reconstructions. Although these technical factors allow for an important reduction of the doses, behavioral factors such as respecting the indications and limitations of the scan coverage remain essential. Finally, we will also indicate how to optimize and reduce the doses in particular applications of musculoskeletal imaging, such as dynamic CT, bone and soft tissue perfusion CT and dual-energy CT.

A. Gervaise · P. Teixeira · S. Lecocq · M. Louis · A. Blum
Guilloz Imaging Department, Hôpital Central, CHU Nancy, 29 avenue du Maréchal de Lattre de Tassigny, 54035 Nancy Cedex, France

A. Gervaise (✉)
Medical Imaging Department, Hôpital d'Instruction des Armées Legouest, 27 avenue de Plantières, BP 90001, 57077 Metz Cedex 3, France
e-mail: alban.gervaise@hotmail.fr

N. Villani
Medical Radiophysics Unit, CRAN UMR 7039 CNRS, Centre Alexis Vautrin, Avenue de Bourgogne, 54511 Vandoeuvre-les-Nancy, France

D. Tack et al. (eds.), *Radiation Dose from Multidetector CT*, Medical Radiology. Diagnostic Imaging,
DOI: 10.1007/174_2011_500, © Springer-Verlag Berlin Heidelberg 2012

1 Introduction

Since its introduction in the 1970s, computed tomography (CT) has played an important role in the diagnosis of musculoskeletal disorders. It quickly became the method of choice for the diagnosis of traumatic, degenerative or developmental lesions. Although image quality is altered by streak artifacts of medical devices, CT is still indicated in post-operative imaging (Blum et al. 2000; Cotten et al. 2002; Fayad et al. 2005). Today, CT is also widely used in interventional imaging (i.e., guided injection, biopsy, vertebroplasty, etc.) (West et al. 2009).

The diagnostic performance of CT is however limited by the low-contrast resolution, which leads to a poor analysis of soft tissues when compared with magnetic resonance imaging (MRI). The analysis of intra-articular lesions is also very difficult in the absence of intra-articular contrast. CT studies may also be an important source of ionizing radiation. This may help explain the prominent role of MRI in the evaluation of musculoskeletal disorders.

With multi-detector computed tomography (MDCT), wide-range detectors and a significant reduction in radiation exposure, CT has regained its former importance in the evaluation of the musculoskeletal system. Spatial and temporal resolutions were considerably increased. Submillimetric isotropic acquisition allows multiplanar and volume rendering (VR) three-dimensional (3D) reformations, improving the diagnosis and preoperative planning of bone and soft tissues disorders (Iochum et al. 2001). Improvements in temporal resolution limit motion artifacts especially in large-volume explorations, which are particularly suitable for the evaluation of polytraumatized patients with musculoskeletal injuries (Fig. 1). Additionally, high temporal resolution allows dynamic imaging of joints. Novel CT techniques, such as dual-energy and CT perfusion are also available for musculoskeletal imaging. Dual-energy CT is based on image acquisition with a beam with variable kilovoltage allowing not only a better characterization of tissues, but also a reduction in metal artifacts. Bone and contrast media can also be subtracted with this technique (Karcaaltincaba and Aktas 2011). With CT perfusion, multiple and successive phases are acquired allowing an optimal analysis of the contrast bolus. This technique provides a functional evaluation of bone and soft tissues' tumors with the advantages of being more reproducible and easier to analyze than MRI (Oldrini et al. 2009; Goh and Padhani 2006). Other benefits of CT scanning include a lower cost, better availability, fewer contraindications and the possibility to image post-operative or unstable patients (Semelka et al. 2007; West et al. 2009).

Finally, advances in CT technology helps to reduce the radiation exposure. After a review of the typical doses used in musculoskeletal CT examinations, we will discuss in detail the various methods of dose reduction in the field of musculoskeletal imaging, with a special emphasis on both behavioral and technical factors.

2 Typical Doses Used in Musculoskeletal CT Examinations

The International Commission on Radiological Protection (1991) advocates the establishment of recommended doses for CT examinations. When greater exposure is proposed, the need for it, and the implications of its use, should be examined. The Council Directive of June 30, 1997, requests each Member State of the European Union to establish and enforce the use of reference levels of diagnostic radiation exposure that should not be exceeded during standard procedures (European Community 1997). The European Commission proposes reference values of weighted CT Dose Index (CTDIw) and Dose Length Product (DLP) for various types of CT studies (European Commission 1999).

For the lumbar spine, the proposed reference levels are a CTDIw of 35 mGy and a DLP of 800 mGy cm. For the pelvic girdle (i.e., hip, sacroiliac), the proposed reference levels are a CTDIw of 25 mGy and a DLP of 520 mGy cm. For the exploration of a traumatic spine, the proposed values are a CTDIw of 70 mGy and a DLP of 460 mGy cm (European Commission 1999). These reference doses are, however, based on survey data from the late 1980s and early 1990s, prior to the widespread introduction of spiral CT and MDCT (Shrimpton and Edyvean 1998; Hidajat et al. 2001). Since then, MDCT has dramatically changed clinical practice, and the guidelines should be reviewed accordingly (Hidajat et al. 2001; Bongartz et al. 2004).

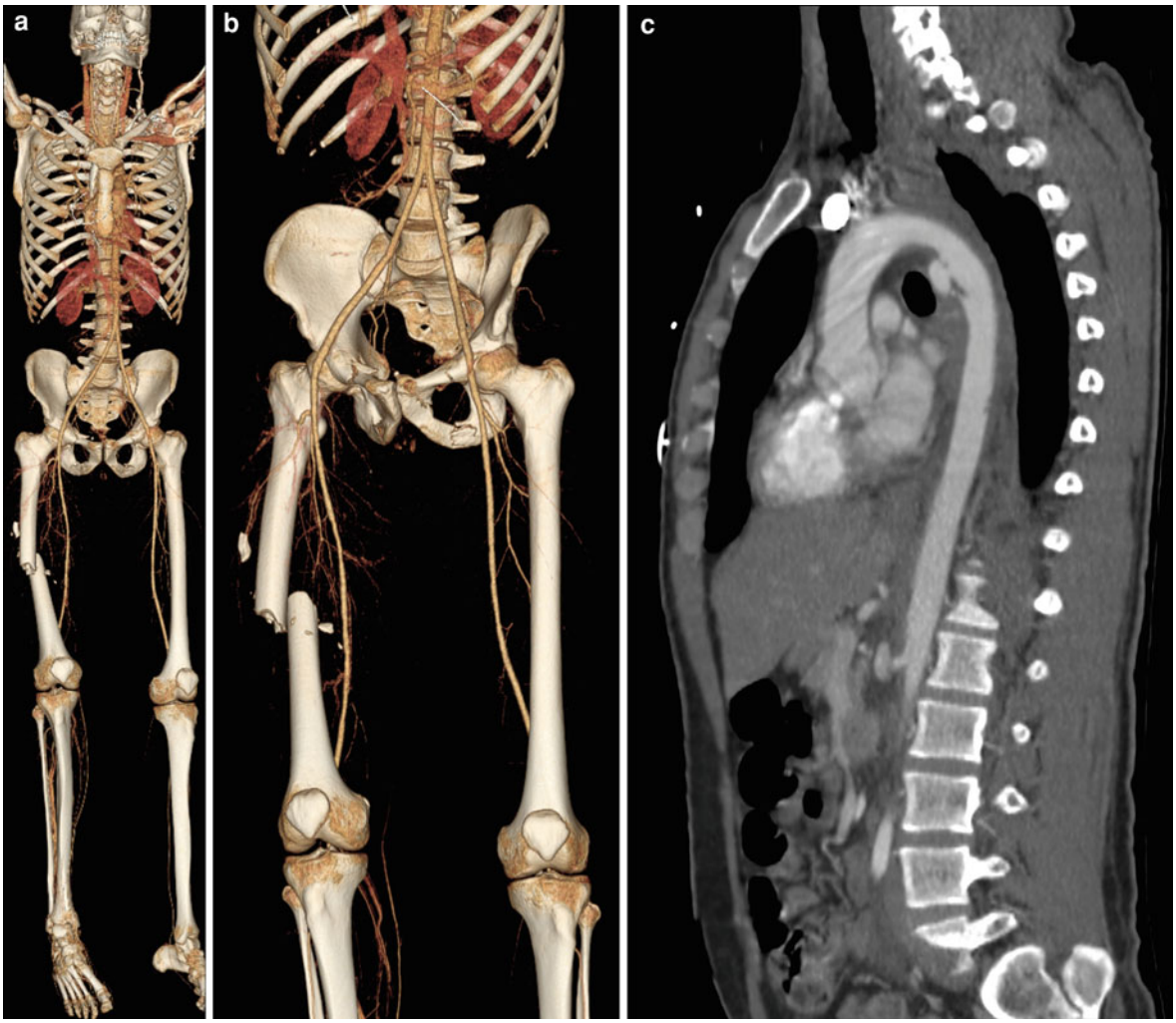

Fig. 1 Whole-body CT-scan of a 28-year-old man for assessment of bike on car polytrauma. Arterial acquisition with 3D reformations in VR of the whole body (**a**) then centered on the right femoral fracture (**b**) and sagittal oblique reformation of the thoracic aorta (**c**). The acquisition was performed with a 64-detector row CT covering the whole body, representing a 180 cm acquisition in 34 s (64 × 0.5 mm, rotation time 0.5, pitch 0.828, 120 kV, current tube modulation with mAs range 50–145 mAs, DLP = 2,090 mGy cm). This acquisition was performed at the arterial phase with thin slices, allowing for 3D VR vascular reformation. This reformation allows for a better analysis of the ratio between the diaphyseal fracture of the right femur and the superficial femoral artery and to assist in preoperative assessment. Note also the bilateral fracture of the obturator rings and the rupture of the aortic isthmus

For example, it is interesting to note that these guidelines recommend a nominal slice thickness of 2–5 mm for a lumbar spine CT, while most MDCT acquisitions today are systematically performed with submillimetric slice thicknesses. Moreover, due to the improvement of MDCT acquisition speed, it is now possible to obtain a wide *z*-axis coverage, which leads to new indications, such as whole-body bone CT for the assessment of a myeloma (Horger et al. 2005; Gleeson et al. 2009) or whole-spine CT for the assessment of osteoporosis (Damilakis et al. 2010). The new techniques made possible by the developments in CT technology, such as dynamic imaging, perfusion and dual-energy still do not have established dose reference levels. Finally, the dose exposure of CT studies in some parts of the musculoskeletal system (such as peripheral joints) either has not yet been evaluated or has no reference dose values determined (i.e., shoulder).

Table 1 Spine CT scan doses from a literature review (Pantos et al. 2011)

Spine segment	CTDIw[a] (mGy)	DLP[a] (mGy cm)	Effective Dose[a] (mSv)
Cervical	44.3 (5.3–103.2)	324 (56–1,275)	2.6 (0.3–7.5)
Thoracic	NA	253 (66–515)	4.6 (1.0–9.8)
Lumbar	30.3 (10.6–59.7)	302 (49–870)[b]	5.2 (0.8–15.7)

NA not available

[a] Values are given as the median, and range values are in parentheses

[b] Note the differences between lumbar spine CT doses given by Pantos et al. (2011) and Biswas et al. (2009) in Table 2. This differences can be principally explained by the increase in dose between single detector CT and MDCT [Pantos et al. (2011) mainly refers to surveys performed on single detector CT while Biswas et al. (2009) performed its study on MDCT] and also reflect the increase in *z*-axis coverage supported by faster acquisitions with MDCT

In the literature, publications addressing CT scan radiation doses are still rare, and the results described are variable. In a literature review from 2008, Mettler et al. (2008) reported an average effective dose of 6 mSv for spine CTs, with values ranging from 1.5 to 10 mSv. In a more recent literature review, Pantos et al. (2011) reported an even higher range, from 0.8 to 15.7 mSv for a lumbar spine CT, with a median dose of 5.2 mSv (Table 1). On the other hand, a study focusing on musculoskeletal CT doses, Biswas et al. (2009) revealed an average dose of 19.15 mSv in their institution for the acquisition of lumbar spine CT (Table 2). This large dose variability can mainly be explained by the difference in the *z*-axis coverage between these studies. For example, Galanski et al. (2001) reported an average dose of 2.7 mSv with an average coverage of only 5.8 cm with a single-slice CT scanner. Biswas et al. (2009) on the other hand reported an average dose of 19.15 mSv, for an average coverage of 25.5 cm, with a 16-detector row CT scanner. These differences in the delivered radiation dose are more related to the CT acquisition protocol used, rather than a difference in the number of detectors rows. Although the change from single-slice CT to MDCT implied in an increase of the delivered dose (Thomton et al. 2003), the switch from 4 to 16 or 64-detector row CT did not. The technical improvements that accompanied the increase of detector rows keep the delivered dose relatively stable (Mori et al. 2006; Jaffe et al. 2009; Fuji et al. 2009). In fact, the increase in the overall number of CT scans performed (Brenner and Hall 2007) as well as the increase in *z*-axis coverage supported by faster acquisitions lead to increased radiation exposure (Mettler et al. 2008; Richards et al. 2010). Furthermore, within a single institution, significant variations regarding CTDI and DLP are also observed (Tables 2 and 3). This can be explained by the adjustment of exposure parameters according to patient size and CT indication. For example, tube output parameters are kept low for the evaluation of bony structures, whereas for a focused soft tissue evaluation it is necessary that the tube output has to be increased. Implementation of new dose reduction techniques, such as iterative reconstruction, also influences the dose delivered during CT-scan (Table 3).

Very few studies report CT exposure levels on peripheral joints. To our knowledge, the only study analyzing all the doses delivered in musculoskeletal CT, including peripheral joints, was performed by Biswas et al. (2009). Their results showed that with respect to the radiation exposure on CT the farther from trunk the lower the effective dose, which was almost negligible for wrist studies (Table 2). This is due to the fact that peripheral joints are small in size, so tube output parameters and *z*-axis coverage can be shortened. In addition, the tissue weight coefficient used to calculate the effective dose is very small in view of the absence of nearby radiosensitive organs. Table 4 summarizes the values of the tissue weights used by Biswas et al. (2009) to estimate the effective dose in musculoskeletal CT in various anatomic locations.

3 Modalities for Dose Reduction in Musculoskeletal CT

The rational for CT dose reduction arises from three major principles of radioprotection: justification, optimization and substitution (International Commission on Radiological Protection 1977). These principles have notably been included in the European directive Euratom 97/43 (European Community 1997)

Table 2 Upper and lower extremity joint and spine exposure data for computerized tomography (Biswas et al. 2009)

Joint scan	CTDIvol[a] (mGy)	DLP[a] (mGy cm)	Effective dose[a] (mSv)
Wrist and hand	14.41 ± 15.52	137 ± 134	0.03 ± 0.03
Elbow[b]	21.52 ± 23.83	293 ± 311	0.14 ± 0.22
Shoulder	19.49 ± 13.77	316 ± 211	2.06 ± 1.52
Hip	19.83 ± 7.67	422 ± 174	3.09 ± 1.37
Knee	18.39 ± 14.43	360 ± 288	0.16 ± 0.12
Ankle and foot[c]	17.88 ± 13.39	310 ± 210	0.07 ± 0.05
Cervical spine	64.17 ± 29.04	1,414 ± 831	4.36 ± 2.03
Thoracic spine	64.39 ± 22.23	2,171 ± 805	17.99 ± 6.12
Lumbar spine	66.53 ± 21.56	1,701 ± 689	19.15 ± 5.63

[a] The values are given as the mean ± the standard deviation
[b] Arm only (arm above the head)
[c] Unilateral

Table 3 Lumbar spine CT and shoulder CT-arthrography doses in the present authors' institution before and after implementation of iterative reconstructions Adaptive Iterative Dose Reduction 3D (AIDR 3D, second version of Toshiba CT iterative reconstruction)

	CTDIvol[a] (mGy)	DLP[a] (mGy cm)	Effective dose[a] (mSv)
Lumbar spine CT			
Before iterative reconstruction[b]	40.2 ± 11.4	1,094 ± 309	12.32 ± 3.5
With AIDR 3D	25.5 ± 11.9	695 ± 338	7.83 ± 3.8
Shoulder CT-arthrography			
Before iterative reconstruction[b]	43.9 ± 15.9	611 ± 260	3.98 ± 1.7
With AIDR 3D	16.1 ± 4.3	205 ± 82	1.34 ± 0.5

[a] The values are given as the mean ± standard deviation
[b] CT-scans performed in Filtered Back Projection with Quantum Denoising System (Toshiba)

Table 4 Dose conversion factors used to estimate effective doses for different musculoskeletal CT-scan examinations calculated by Biswas et al. (2009)

Joint and spine CT scan	Dose conversion factors[a] (μSv/mGy cm)
Shoulder	6.52
Elbow[b]	0.48
Wrist and hand	0.22
Hip	7.31
Knee	0.44
Ankle and foot[c]	0.23
Cervical spine	3.08
Thoracic spine	8.29
Lumbar spine	11.26

[a] Dose conversion factors are calculated by dividing the effective dose by the dose length product given by the study of Biswas et al. (2009). Note that Biswas et al. calculated these factors with IMPACT dosimetry calculator software according to ICRP 60. New factors should be used to take into account the ICRP 103 values
[b] Arm only (arm above the head)
[c] Unilateral

and in the precautionary principle As Low As Reasonably Achievable (ALARA). The ALARA principles have been widely and repetitively discussed in the literature (Kalra et al. 2004; Semelka et al. 2007; McCollough et al. 2009; Lee and Chhem 2010; Singh et al. 2011; Dougeni et al. 2011). We are going to approach each of these principles successively demonstrating their behavioral implications, technological fundaments and focusing on their application in musculoskeletal CT.

3.1 Behavioral Factors

Awareness and education. First, as in any other field, the level of education and awareness among radiologists and technologists are important elements in the process of dose reduction. Wallace et al. (2010) showed that after educating a physician, it was possible to reduce, by 29%, the lumbar spine CT doses used within several institutions.

Justification and substitution. Justification and substitution are also two important elements, particularly in musculoskeletal CT, where the substitution with imaging methods without ionizing radiation, such as ultrasound or MRI are often possible (Semelka et al. 2007; West et al. 2009; Borgen et al. 2006). For instance, Oikarinen et al. (2009) showed in their study on 30 lumbar spine CT performed on patients younger than 35 years that in only seven (23%) of them the indication could be justified. Among these studies, 20 could have been replaced by MRI, and three patients needed no imaging at all. Clarke et al. (2001) also showed that 90% of lumbar spine CT could have been replaced by MRI. MRI, however, is not always feasible because of patient claustrophobia, incompatible implants, pacemakers or critical medical conditions (Semelka et al. 2007). The performance of CT is, nonetheless superior to that of MRI in some settings (West et al. 2009). In spine imaging, CT shows a better sensitivity for the detection of early infection-related bone changes (Tins et al. 2007). CT is also better than MRI for the characterization of gas and calcifications. Because of its high spatial resolution, CT also allows a better visualization of scaphoid cortical fractures (Memarsadeghi et al. 2006), a better analysis of wrist ligaments lesions when combined with arthrography (Moser et al. 2007) and a better detection of some osteoid osteomas with respect to MRI (Liu et al. 2003). Finally, CT-angiography is sometimes better than MR-angiography for the assessment of vascular invasion from bone and soft tissue tumors (Argin et al. 2009; Thévenin et al. 2010). In our institutions, CT is indicated in the following situations: complex fracture, fracture with vascular impairment, fracture-dislocations, occult fractures (other than hip and scaphoid), bone and soft tissue tumors, postoperative follow-up, bone dysplasia, intervertebral disc herniations and joint evaluation. CT arthrography can be performed in almost any joint and offers a better evaluation of superficial cartilage lesions and multiplanar reformations which can be useful in the preoperative evaluation (Omoumi et al. 2009; Wyler et al. 2009).

Scan coverage and number of phases. During the realization of a scan, the dose can be mastered by reducing the number of acquisitions (i.e., phases) and the length of acquisition in the *z*-axis (Rehani et al. 2000). The coverage must be limited to the zone of interest, previously identified by the scout views. As mentioned above, it is one of the major reasons for dose differences between various examinations ("The smaller the exposed area, the smaller the dose"). In musculoskeletal CT most examinations consist of a single-phase non enhanced acquisition. With the development of interventional, dynamic and perfusion CT, multiple acquisitions are performed in the same area making the limitation of the number of phases important for dose reduction.

Position and centering. A precise centering of the anatomical zone to be scanned in the isocenter of the CT gantry provides optimal image quality and delivered dose (Kalra and Toth 2007). Spatial resolution is better in the isocenter of the gantry because more interpolations of the data are performed than at the periphery (Li et al. 2007). With the increase of the width of the beams, and particularly with 64 or 320-MDCT, cone beams generate more artifacts (Mahesh 2009). These artifacts are less severe in the isocenter of the gantry and are not noticed in practice with a good centering. Moreover, a good centering is particularly important with the use of the automatic dose modulation because the calculations are made considering the patient to be in the isocenter of the gantry. Improper centering can increase the dose significantly (Mahesh 2009). The width of the scanned volume should also be as narrow as possible to limit scattered radiation and beam-hardening artifacts. Therefore, shoulder girdles should be placed on different levels when exploring the shoulder. During acquisitions on the lower limb (i.e., foot, ankle,

knee), the contralateral limb should be flexed out of the scanning field when possible. Additionally peripheral joints should be scanned as far as possible from the trunk of the patient in order to decrease the dose received in radiosensitive organs. Biswas et al. (2009) showed that the acquisition of an elbow alongside the body as compared to above the head was the source of a considerable increase of the effective dose (8.35 vs. 0.14 mSv, respectively).

3.2 Technical Factors

Scan modes. While with the spread of MDCT the helical mode lead to a replacement of the sequential acquisition mode, the development of wide-detector area CT scanners lead to its come back. 320-detector row CT scanners now allow the acquisition of a 16 cm volume, covering the entire length of most joints with a single tube rotation (i.e., shoulder, wrist and hand, hip, sacroiliac, knee, ankle and foot). This scanning mode considerably reduces acquisition time (up to 0.24 s for the acquisition of a 16 cm volume, with no gaps), and hence motion artifacts. Moreover it allows a significant dose reduction with respect to the conventional helical mode. With wide-detector area CT, overbeaming is proportionately less important, compared to 16- or 64-detector row CT scanners (Perisinakis et al. 2009; Mori et al. 2008). In addition, the use of volume mode suppresses the overranging which is characteristic of the helical mode (Gervaise et al. 2010). In helical mode, the additional radiation dose due to overranging increases with the number of detectors and is also proportionally more important for the acquisition of smaller volume lengths (van der Molen and Geleijns 2007), as is the case of peripheral joint acquisitions. Thus, when evaluating small parts with a 16- or 64-detector row CT scanner, some authors suggest using the sequential or step-and-shoot acquisition mode to avoid the additional dose exposure due to overranging (Schilham et al. 2010; Kalra et al. 2004).

Tube potential. Reduction of the tube kilovoltage (kV) accounts for an important dose reduction (for example, keeping other parameters constant, a kilovoltage decrease from 120 to 80 kV reduces the delivered dose by a factor of 2.2 (Mahesh 2009), but it is also responsible for considerable increase in image noise (Kalender et al. 2009). In practice, the increase in noise is not detrimental to the analysis of bone structure, thanks to its high natural contrast. It is therefore possible to image peripheral joints at 80 kV (i.e., wrist, knee, ankle, foot) (Figs. 2, 3). For large proximal joints (i.e., shoulder, hip, sacroiliac, spine), the kV must be adapted to the body habitus of the patient: 120 kV for a standard patient, 100 kV for thin patients, and 135–140 kV for patients with excess weight to maintain adequate image quality. For proximal joint CT-arthrography, it is better to use a maximal kilovoltage of 120 because the density of the iodine at 120 is higher than at 140 kV, which can improve the contrast-to-noise ratio (Subhas et al. 2010). During vascular or perfusion examinations, a lower kV of 100 or even 80, depending on the thickness of the anatomical zone to cover, is possible (Nakaura et al. 2011). Some teams also proposed low-dose acquisitions at 100 kV for spinal traumas (Mulkens et al. 2007) or myeloma (Kröpil et al. 2008) assessment. Acquisitions with kV as low as 80 have been advocated for scoliosis (Abul-Kasim et al. 2008) or osteoporosis assessment (Damilakis et al. 2010).

Tube current and mAs. The reduction in milli-Amperage (mA) causes a proportional decrease of the delivered dose, but also an increase in image noise. This can be deleterious to the interpretation of the CT-scans which require a good contrast-to-noise ratio, as is the case for discoradicular pathologies. In their study on lumbar spine CT, Bohy et al. (2005) showed that a mAs reduction beyond 35% of the standard settings lead to a decrease in the diagnostic performance of lumbar spine CT. Today, the development of automatic dose modulation allows the adaptation of the mA to the patient's body habitus (McCollough et al. 2006). Van Straten et al. (2009) showed that this type of modulation was particularly interesting in some anatomical regions such as shoulders and pelvis, where it accounted for an effective dose reduction of 11 and 17%, respectively. Its use is also interesting to adapt the mA to the variations in the patient's body habitus when long body segments are imaged (e.g. lumbar spine) while keeping a homogeneous image quality. Mulkens et al. (2005) showed that the use of automatic dose modulation in three-dimension (3D-AEC) allowed for a dose reduction of 37% in lumbar spine CT studies. Mastora et al. (2001) also found that online tube current modulation resulted in a 35% reduction in the product of mean tube current and time with no loss in image quality when exploring the thoracic outlet for

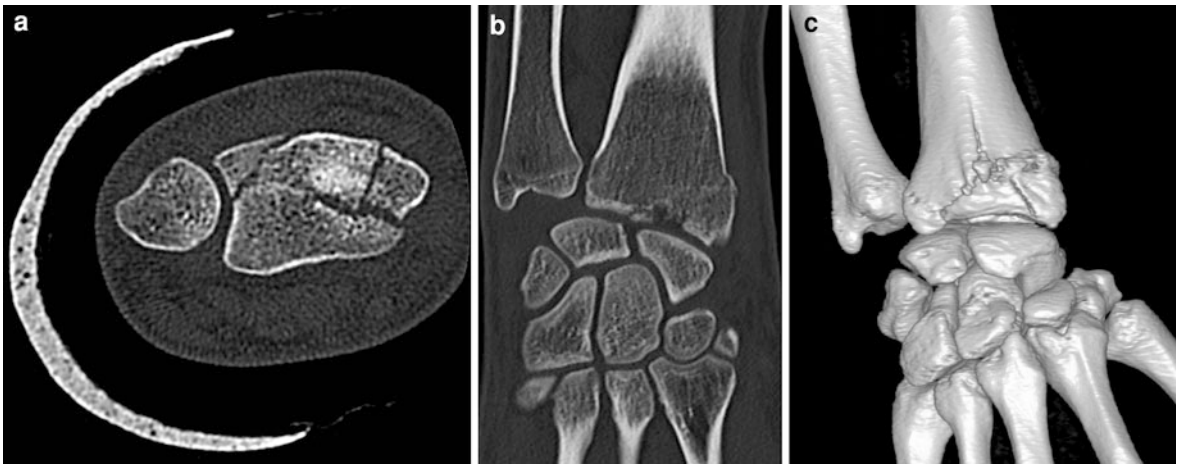

Fig. 2 CT-scan of the right wrist of a 20-year-old man during the preoperative assessment of a parachute trauma with 0.5 mm axial slices in bone window centered on the distal extremity of the radius (**a**), coronal reformation in bone window in 1.5 mm slice (**b**), and 3D reformation in VR (**c**). Note the good analysis of the bone structures thanks to coronal and 3D reformations in spite of the important reduction of the acquisition parameters (volume acquisition in 200 × 0.5 mm, 80 kV, 50 mAs, rotation time 0.5 s) and scan dose (DLP = 39.3 mGy cm and effective dose = 0.008 mSv). In comparison, this CT dose is only 21 times more than a standard wrist radiographic examination (0.38 μSv) (Noel et al. 2011)

Fig. 3 CT-arthrography of the right knee of a 64-year-old woman presenting with post-traumatic pain by rupture of a popliteal cyst. Axial slice centered on the patellofemoral joint acquired in volumic scan mode with 80 kV, 50 mAs, rotation time 0.5 s and with DLP = 15.3 mGy cm. Note the good visualization of the patellofemoral chondropathy in spite of the important reduction of the acquisition parameters

suspected thoracic outlet syndrome. Moreover, some authors proposed low-dose protocols with low mA. Horger et al. (2005) showed that whole-body low-dose MDCT is appropriate for the diagnosis of lytic bone lesions and for the assessment of fracture risk in multiple myeloma patients. In their study, a 16 × 1.5 mm collimation was used with a tube voltage of 120 kV and a tube current time product ranging from 40 to 70 mAs. The effective dose of MDCT calculated with a tube current time product of 40 mAs was only 1.7-fold higher than the mean radiation dose associated with whole-body conventional X-ray (4.1 vs. 2.4 mSv) (Horger et al. 2005).

Pitch. With some current MDCT using the concept of effective mAs (mAs/pitch), pitch modification has no influence on the dose because it is automatically adapted to mA (Nagel 2007). A high pitch, of about 1.5, is preferred to reduce the acquisition time and motion artifacts (for example, during the exploration of a polytraumatized patient). The pitch should, however, remain lower than 2 to keep an optimal quality of multi-planar reformations (Nagel 2007) and to avoid helical artifacts (Kalra et al. 2004). In contrast, a small pitch is preferred to reduce metal hardware-related artifacts (Stradiotti et al. 2009).

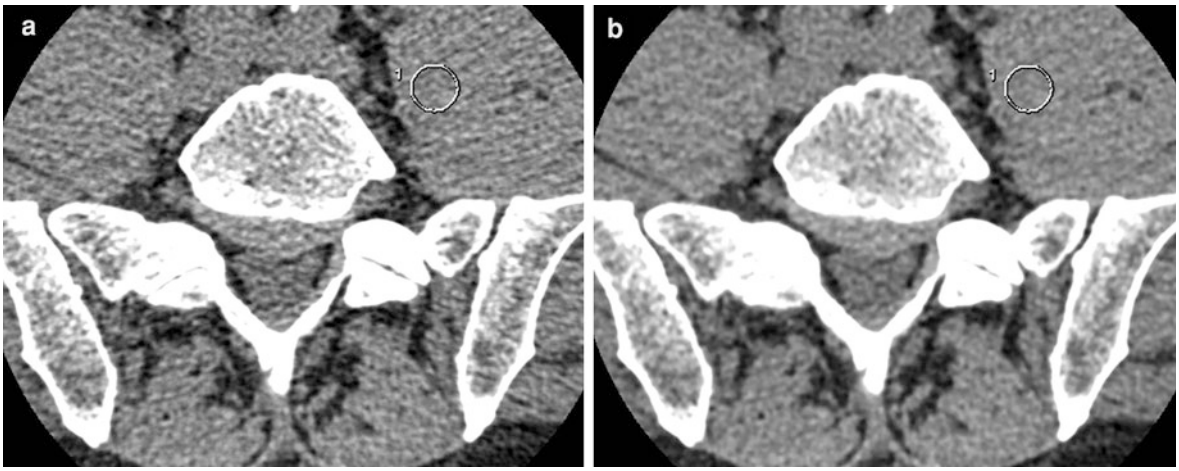

Fig. 4 Transverse lumbar spine CT images reconstructed with standard filtered back projection (FBP) (**a**) and Adaptive Iterative Dose Reduction 3D (AIDR 3D) (**b**) in a 56-year-old man (1 mm slices, 135 kV, tube current modulation with noise index set at 8, DLP = 347 mGy cm). Note the noise reduction with AIDR 3D compared to FBP, without any significant change in image pattern (standard deviation values of the ROIs placed in left psoas muscles are 27.94 HU with FBP and 18.39 HU with AIDR 3D, which corresponds to a noise reduction of 34%)

Slice thickness. In general, acquisitions are performed with thin slices (0.5–1 mm) required for bone structure analysis and reconstructed in thicker slices (2–5 mm) for soft tissues analysis. Submillimetric slices improve spatial resolution, reduce partial volume effects and allow the reconstruction in a quasi-isotropic volume (von Falck et al. 2010). On the other hand, thin slice acquisition can lead to an increased radiation dose to the patient (McNitt-Gray 2002). In case of excessive mA reduction, the acquisition in thin slices engenders an increase in image noise. So, whereas the acquisition is made in submillimetric slices, the soft tissues analysis is performed on thick slices with a better signal-to-noise ratio (von Falck et al. 2010).

Iterative reconstruction. The use of iterative reconstruction is a considerable advance in terms of CT dose reduction (Table 3). The first result showed a dose reduction of at least 50%, while keeping an equivalent image quality (Hara et al. 2009; Silva et al. 2009). Few studies have focused on the evaluation of the benefits of iterative reconstruction in musculoskeletal imaging. In our institution, we conducted a study on 15 lumbar spine CT acquired in volume mode with a 320-detector row CT scanner. The images acquired using iterative reconstruction (Adaptive Iterative Dose Reduction—AIDR, first version of Toshiba CT iterative reconstruction) were compared to those acquired using standard filtered back projection (FBP) (Gervaise et al. 2011). Image noise and signal-to-noise ratio (SNR) were quantified, measuring the values of the regions of interest (ROI) placed in similar anatomic regions on both AIDR and FBP series. A subjective analysis of the image quality was performed by two radiologists. Our results showed a significant reduction of 31% (24–37%) of the mean image noise with AIDR, compared with FBP images and an improvement of 47% (33–63%) of the mean SNR. The qualitative evaluation also showed a significant improvement of the image quality on the AIDR series when compared with FBP images. Despite the image noise reduction, there was no modification of spatial resolution. Finally, our study showed a mean potential dose reduction of 52% with AIDR compared to FBP. These preliminary results are promising, and even more so, as iterative reconstructions continue to quickly evolve (Fig. 4).

Whereas iterative reconstruction is particularly interesting to reduce the dose of examinations maintaining a good SNR, it is less useful in cases directed primarily to bone analysis, for example in search of a fracture. The high natural contrast of bone structures allows low-dose acquisitions sometimes noisy, but with no affect on the interpretation. However, one of the other main advantages of iterative reconstruction is the reduction of artifacts associated with beam hardening and FBP (Boas and Fleischmann 2011) (Fig. 5). It is thus particularly interesting for bone and soft tissues analysis when metal hardware is present. Traditionally,

Fig. 5 Shoulder CT images reconstructed with standard filtered back projection (FBP) (**a**, **b**) and Adaptive Iterative Dose Reduction 3D (AIDR 3D) (**c**, **d**) in a 59-year-old man. 0.5 mm axial slices (**a**, **c**) and 0.5 sagittal reformations (**b**, **d**) in bone windowing. Note the noise reduction with AIDR 3D compared to FBP associated with a reduction of streak artifacts (volume acquisition in 240 × 0.5 mm, 120 kV, 150 mAs, rotation time 0.75 s, DLP = 151 mGy cm and effective dose = 1 mSv)

a better visualization of metallic materials requires the increase of parameters such as the kVp and the mAs, as well as a low pitch and a thin collimation. All these parametric changes are a source of dose increase. Iterative reconstruction reduces the metal and the streak artifacts while avoiding a dose increase due to the optimization of the acquisition parameters.

Noise reduction filter. The improvement of the SNR necessary for the analysis of soft tissue, particularly in discoradicular pathology, can also be made by the use of noise reduction filters with a post-processing software. The application of these filters is performed on already-reconstructed images, and can be used with any CT image and even 3D reformations. Contrary to filters used during the process of image reconstruction, some of these noise reduction filters seem to smoothen the image without altering spatial resolution. However, studies should be performed to confirm the benefits of these new post-treatment software packages.

Overranging shield. These shields reduce the overranging by using an active collimation in the *z*-axis at the beginning and at the end of the helical CT scan (Stierstorfer et al. 2007). They are particularly interesting for the study of small length body parts with a 16- or 64-detector row CT when overranging is an important factor affecting the radiation dose delivered

to the patient. Christner et al. (2010) showed that with a 64-detector row CT, with a pitch of 1, a total nominal beam width of 38.4 mm and an acquisition length of 15 cm, the dose reduction with a shield reached up 16% of the total dose delivered. On the other hand, for acquisitions with a coverage of more than 300 mm in a 64-detector row CT scanner, overranging represented less than 3% of the total dose, whichever pitch was used (Christner et al. 2010). In musculoskeletal CT, this active collimation is thus particularly efficient to reduce the dose during the acquisition with a 16- or 64-detector CT-scan of the shoulders and hips, considering the short coverage and the proximity of radiosensitive organs (i.e., the thyroid and gonads).

4 Dynamic Studies of Joint Motion

A study of motion can be performed by the mean of multiple static acquisitions at different joint position or as a continuous dynamic acquisition. This latter must be privileged during motion studies of joints (Wolfe et al. 2000; Moojen et al. 2003; Foumani et al. 2009) not only because the constraints are different between a moving and a static system but also because the phenomenon of hysteresis can influence the position of various anatomical structures (Berdia et al. 2006; Short et al. 1997). The improvement of the temporal resolution of MDCT and the development of wide-detector area CT scanners allow dynamic studies of peripheral joints (Hristova et al. 2009; Blum et al. 2009). The adaptation of the acquisition parameters, as well as the application of recent methods of dose reduction help to maintain a low radiation dose. Thus, CT becomes a functional analysis tool, improving the analysis of in vivo articular motion and joint dysfunction.

A dynamic motion study is possible in helical mode with a 64-detector row CT scanner. Tay et al. (2007) showed in an experimental study that it was possible to perform the motion acquisition of a wrist in four phases with a very low pitch (0.1) by using a protocol with retrospective gating. This technique, however, creates many motion and band artifacts as well as an important increase in radiation dose (Tay et al. 2007), making it a lot less efficient than volume acquisitions with wide-detector CT scanners.

In our institution, we study the motion of joints with a 320-detector row CT, allowing the acquisition of volumes up to 16 cm in length. A tube rotation speed of 0.35 s combined with a partial reconstruction technique of the data warrants a temporal resolution as low as 0.24 s. This volume acquisition mode also presents some advantages: reduction of the dose compared to the helical mode (Gervaise et al. 2010) and the temporal uniformity of the acquired volume (every single voxel acquired at the same time with no table movement and no gaps). Using this technique, we are able to evaluate joint motion in several clinical settings: wrist occult instabilities, patellofemoral pain syndromes, posterior impingement of the ankle and subtalar joint motion analysis (Fig. 6).

These motion studies require the repetition of several acquisitions, which leads to increased radiation dose. On a peripheral joint however, performing low-dose acquisition with an effective dose lower than 1 mSv without compromise to the interpretation of the motion is possible (Snel et al. 2000). For the flexion/extension study of the wrist with an acquisition in volume mode of eight phases (80 kV, 17 mAs, rotation time of 0.35 s, scan length of 10 cm), the DLP is only 133 mGy cm, corresponding to an effective dose of 0.1 mSv (Fig. 7). Thanks to this low effective dose, it is possible to study several types of movements (i.e., flexion/extension, clenching the fist, ulnar and radial deviations), while keeping a total effective dose largely below 1 mSv.

For the dynamic exploration of the hip or the shoulder, it is important to reduce radiation dose by optimizing the scan parameters. If the motion study concerns only the bone segments, the high natural contrast of the bone allows for considerable reduction in kV and mAs (Gurung et al. 2005). It is also important to reduce and center the zone of interest. Even though Hristova et al. (2009) showed improvement of the image quality by continuous acquisition of data, the intermittent acquisition mode is preferred. In this mode the number of phases are generally limited to 12 allowing the reduction in radiation dose by reducing the exposure time. On the pelvis, the radiation dose can be maintained under 10 mSv, which corresponds to that of a standard multiphasic abdominopelvic CT.

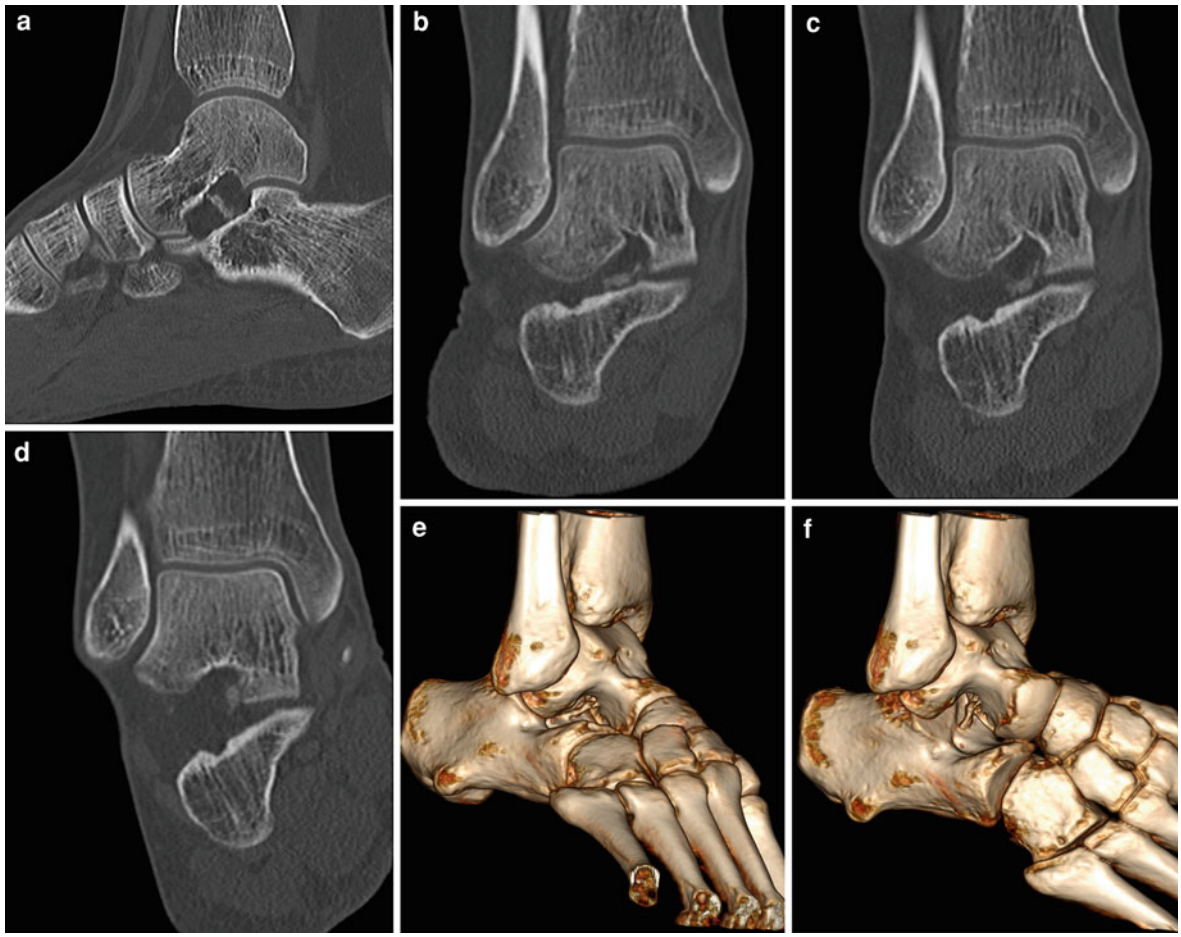

Fig. 6 Dynamic CT scan of the subtalar joint of the right ankle of a 39-year-old woman presenting with a calcification of cervical ligament of the sinus tarsi. Examination performed with a 320-detector row CT with acquisition of seven dynamic phases during eversion/inversion motion of the ankle (120 kV, 75 mAs, rotation time 0.5 s, DLP = 811 mGy cm, corresponding to an effective dose of 0.6 mSv). Sagittal reformation on the subtalar joint shows the ligament calcification (**a**). Coronal reformations focused on the subtalar joint during the eversion/inversion motion of the ankle (**b**–**d**) and 3D VR reformations in eversion (**e**) and inversion (**f**) showing the range of motion of the right ankle. In spite of the ligament calcification, this dynamic study shows a conservation of the articular range of motion

5 Perfusion Studies

The tumor perfusion with CT-scan was described several years ago (Levine and Neff 1983). Similar to dynamic examinations, CT perfusion of bone and soft tissue tumors are possible due to the improvement of the MDCTs' temporal resolution and the development of wide-detector area CT scanners. CT perfusion studies provide data comparable to that of an MRI on tumoral vascularity, with a better visualization of bone reactive changes (periosteal apposition, cortical fracture, osteolysis) and tumoral neovascularization. The quantification of the enhancement is also easier on CT perfusion when compared to MRI perfusion (Miles et al. 2001). Perfusion studies can be performed in helical mode with MDCT scanners with bidirectional scanning (Ketelsen et al. 2010) or in volume mode with a wide-detector area CT scanners. Tumor perfusion in volume mode, without table movement, can reduce motion artifacts and improve the quality of the reconstructions and perfusion curves. This technique also allows the use of the first acquisition as a bone subtraction mask, thus

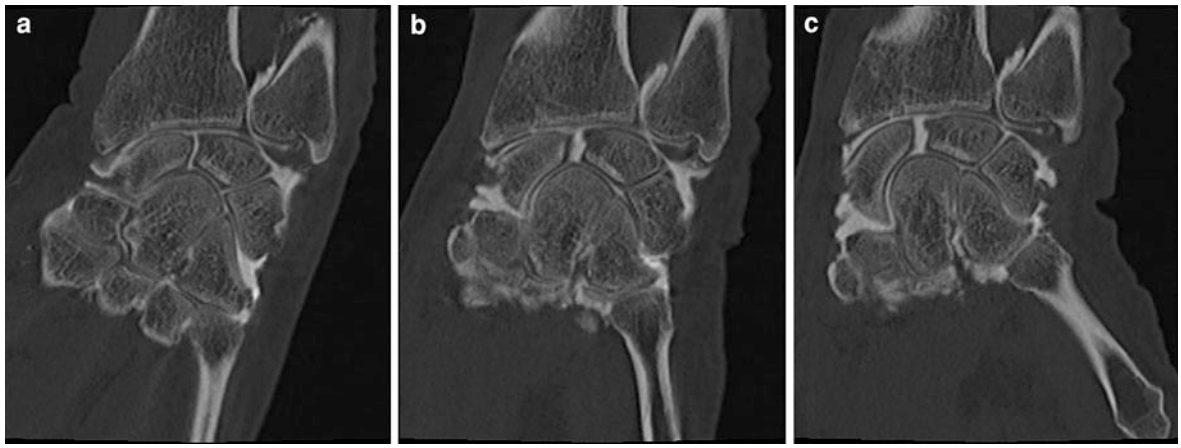

Fig. 7 Dynamic CT-arthrography of the left wrist of a 57-year-old man presenting with scapholunate and luno-triquetral ligament tears. Examination performed with a 320-detector row CT during a radio-ulnar deviation motion with successive acquisitions of eight volumes (scan length of 10 cm, 80 kV, 17 mAs, rotation time of 0.35 s, corresponding to an acquisition time of 2.8 s, DLP = 133 mGy cm and an effective dose of approximately 0.1 mSv). Frontal reformations in 1.5 mm slices: in radial deviation (phase 1: **a**), in neutral position (phase 3: **b**) and in ulnar deviation (phase 5: **c**). Note the increase of the scapho-lunate gap with the ulnar deviation of the wrist

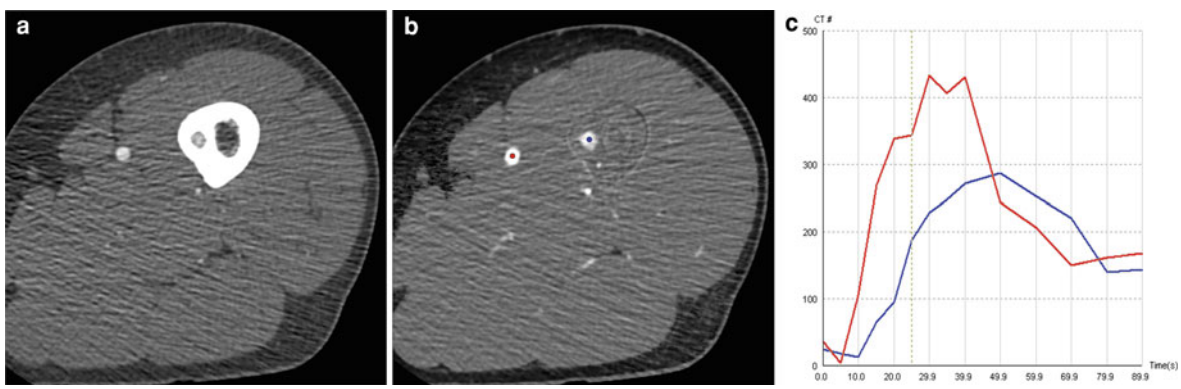

Fig. 8 Tumor perfusion CT of an osteoid osteoma in the left femoral diaphysis of a 38-year-old patient, with 0.5 mm axial slice after contrast injection at the arterial phase, without (**a**) and with bone subtraction (**b**). Perfusion curves of the left superficial femoral artery (*red*) and of the nidus (*blue*) (**c**). The acquisition was performed with a 320-detector row CT with a 16 cm coverage, with 15 phases (first phase without injection, then nine phases every 5 s and five phases every 10 s), 120 kV, 75 mAs and rotation time of 0.5 s, DLP = 495 mGy cm. Note the good visualization of the nidus thanks to the bone subtraction images, confirming the early arterial contrast enhancement also shown by the CT tumor perfusion curve

improving the detection and characterization of intra-osseous abnormalities. However, these perfusion studies lead to an important increase in radiation dose (Ketelsen et al. 2010). The protocol optimization should be performed by adapting the parameters of acquisition (reduction of the kV and the mAs), by reducing the coverage of the scanned area and by limiting the number of acquisition phases.

In our institution, for example, we studied the benefits of CT perfusion for the diagnosis and the follow-up of osteoid osteomas (Heck et al. 2010). A pathology in which MRI findings may be misleading (Liu et al. 2003), and for which CT can facilitate the diagnosis by showing the bone reaction around a small nidus. In addition to characterization of the lesion, the CT perfusion highlights the hypervascularization of the

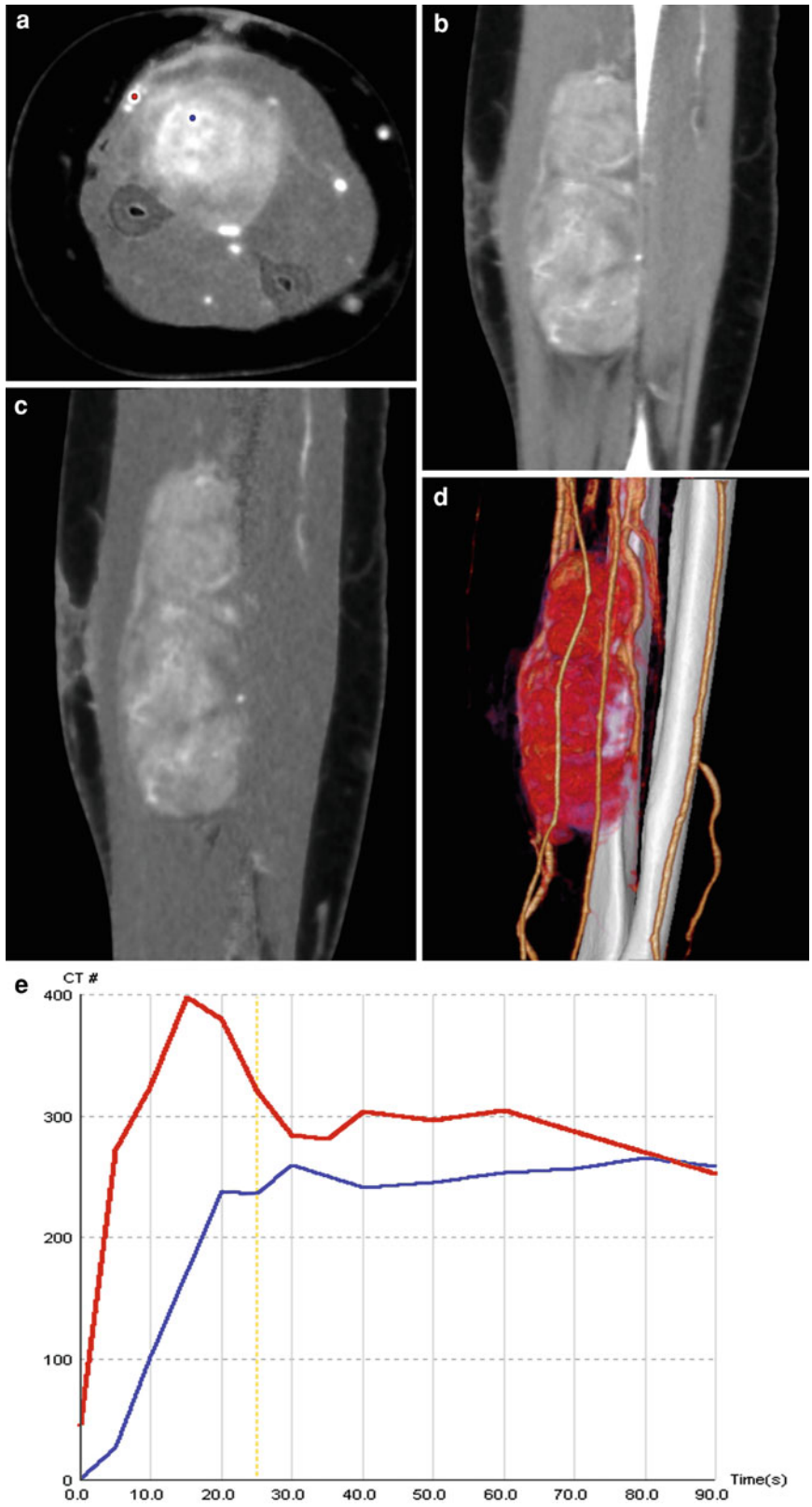

Fig. 9 Tumor perfusion CT-scan of a schwannoma of the forearm in a 51-year-old woman. 0.5 mm axial slice, at the arterial phase (**a**), sagittal reformation without (**b**) and with bone subtraction (**c**), 3D reformation in VR (**d**) and analysis of the perfusion curves by post-processing software (**e**). The acquisition was performed with a 320-detector row CT in volume mode with 240 × 0.5 mm, 12 cm coverage, 80 kV, 50 mAs and rotation time of 0.5 s, acquisition of a first phase without injection, then an intermittent acquisition of nine phases every 5 s, then of five phases every 10 s. The total DLP for 15 phases is 590 mGy cm. The vascular reformations allow for a better analysis of the ratio between the tumor and the vessels and to assist in preoperative planning. The perfusion curves allow for a better analysis of the tumor angiogenesis

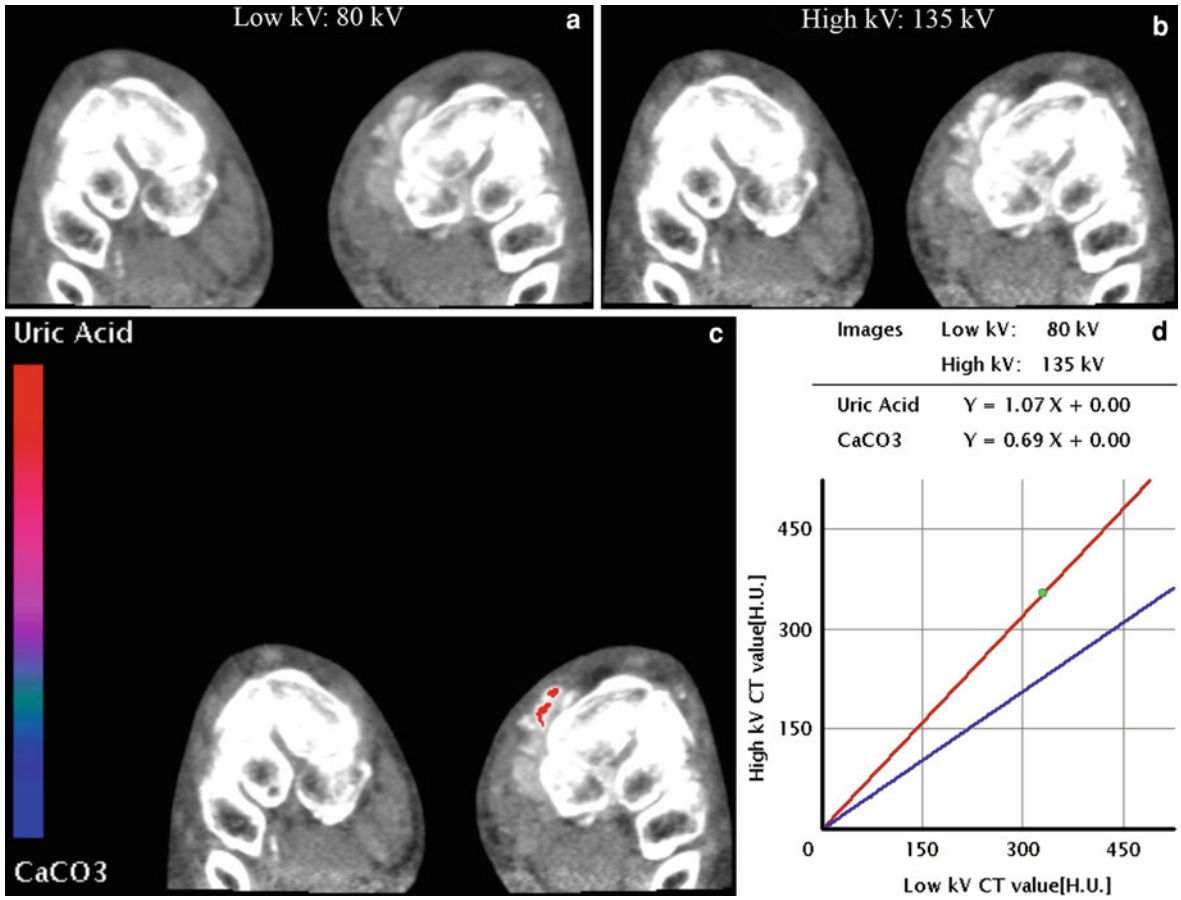

Fig. 10 Dual-energy CT of a 66-year-old man with tophaceous gout of the feet. Examination performed with a 320-detector row CT with acquisition of two successive volumes of 16 cm focusing on feet/ankles and hands/wrists in 80 kV/217 mAs (**a**) and 135 kV/37 mAs (**b**) (collimation of 320 × 0.5 mm, rotation time of 0.75 s). The total dose is 397 mGy cm, corresponding to an effective dose of 0.09 mSv. Post-processing (**c** and **d**) allows for the characterization of the urate deposits by differentiating them from calcifications, thus confirming the diagnosis of tophaceous gout

nidus. A precontrast mask volume can be subtracted from the subsequent injected volumes removing cortical and trabecular bone and helping to demonstrate bone medullary edema-like changes around the nidus. Thus, this additional information, usually provided by MRI, is now accessible through CT scans. To control the radiation dose, we limit the coverage area of the scanner to the zone of interest (approximately 4–8 cm). Moreover, kV and mAs are adapted to the body habitus of the patient and to the anatomical zone. The number of phases is also limited to 15, with an acquisition interval of 5 s for the first nine phases (arterial phase), and then of 10 s for the latter phases. All these measures provide a perfusion study with a total DLP usually between 500 and 800 mGy cm (Figs. 8 and 9).

6 Dual-Energy CT

All manufacturers provide dual energy acquisition on their CT scanners. The techniques used among them are however, quite different. This might have an influence on the results and on the clinical applications of these techniques. Dual-energy CT has several potential applications in the evaluation of musculoskeletal disorders but further studies are still necessary to fully assess its performance (Karcaaltincaba and Aktas 2011).

One application concerns the detection and characterization of urate deposits in gout (Choi et al. 2009). An initial study by Nicolaou et al. (2010) with a dual-source CT scanner showed that the acquisition

of all peripheral joints (elbows, wrists, hands, knees, ankles and feet) provides a good sensitivity and specificity for the detection and the location of tophaceous gout with a total effective dose that varied between 2 and 3 mSv. With the 320-detector row CT, a dual-energy technique is obtained from the successive acquisition of two volumes at different kVp acquired without table feed (the first acquisition with a high kilovoltage and a low milliamperage and the opposite for the second). Thanks to post-treatment software, this method differentiates the deposits of gout from simple calcium deposits, while keeping a low total effective dose (Fig. 10).

Another application of dual-energy CT is bone removal during reconstruction, allowing the identification of bone marrow edema. Pache et al. (2010) showed that it is possible to see a post-traumatic bone marrow edema on knee dual-energy CT, with an increase of the radiation of approximately 28% compared with single-energy CT.

Finally, Subhas et al. (2010) showed that compared to a single-energy acquisition dual-energy CT provides a better signal-to-noise ratio relationship on CT-arthrography of the shoulder with an equivalent dose.

7 Conclusion

CT is an ever evolving imaging modality that remains an important tool for the evaluation of musculoskeletal disorders. Although further studies are still necessary to ascertain the optimal delivered dose, the developments in CT technology lead to a major reduction of patient exposure. The dose reduction techniques discussed, not only allow the acquisition of high quality images with minimal dose, but also open the possibility for new CT applications. Novel techniques such as dual energy CT or CT perfusion often requires extended volume exploration and/or multiphasic acquisitions not feasible previously due to radiation exposure limitations in clinical examinations.

References

Abul-Kasim K, Gunnarsson M, Maly P, Ohlin A, Sundgren PC (2008) Radiation dose optimization in CT planning of corrective scoliosis surgery: a phantom study. Neuroradiol J 21:374–382

Argin M, Isayev H, Kececi B, Arkun R, Sabah D (2009) Multidetector-row computed tomographic angiography findings of musculoskeletal tumors: retrospective analysis and correlation with surgical findings. Acta Radiol 50: 1150–1159

Berdia S, Short WH, Wermer FW, Green JK, Panjabi M (2006) The hysteresis effect in carpal kinematics. J Hand Surg Am 31:594–600

Biswas D, Bible JE, Bohan M, Simpson AK, Whang PG, Grauer JN (2009) Radiation exposure from musculoskeletal computerized tomographic scans. J Bone Joint Surg Am 91:1882–1889

Blum A, Lecocq S, Roch D, Louis M, Batch T, Dap F, Dautel G (2009) Etude cinématique du poignet en 3D et 4D avec un scanner 320 canaux. In: SIMS Opus XXXVI. Poignet et main, éd Sauramps médical, Montpellier, pp 375–389

Blum A, Walter F, Ludig T, Zhu X, Roland J (2000) Multislice CT: principles and new CT-scan applications. J Radiol 81:1597–1614

Boas FE, Fleischmann D (2011) Evaluation of two iterative techniques for reducing metal artifacts in computed tomography. Radiology 259:894–902

Bohy P, de Maertelaer V, Roquigny A, Keyzer C, Tack D, Genevois PA (2005) Multidetector CT in patients suspected of having lumbar disk herniation: comparison of standard-dose and simulated low-dose techniques. Radiology 244:524–531

Bongartz G, Golding SJ, Jurik AG et al (2004) European guidelines for multislice computed tomography. Funded by the European Commission (Contract number FIGMCT2000- 20078-CT-TIP), Mar 2004

Borgen L, Ostense H, Stranden E, Olerud HM, Gudmundsen TE (2006) Shift in imaging modalities of the spine through 25 years and its impact on patient ionizing radiation doses. Eur J Radiol 60:115–119

Brenner DJ, Hall EJ (2007) Computed tomography an increasing source of radiation exposure. N Engl J Med 357:2277–2284

Choi HK, Al-Arfaj AM, Eftekhari A, Munk PL, Shojania K, Reid G, Nicolaou S (2009) Dual energy computed tomography in tophaceous gout. Ann Rheum Dis 68:1609–1612

Christner JA, Zavaletta VA, Eusemann CD, Walz-Flannigan AI, McCollough CH (2010) Dose reduction in helical CT: dynamically adjustable z-axis X-ray beam collimation. Am J Roentgenol 194:W49–W55

Clarke JC, Cranley K, Kelly BE, Bell K, Smith PH (2001) Provision of MRI can significantly reduce CT collective dose. Br J Radiol 74:926–931

Cotten A, Iochum S, Blum A (2002) 3D imaging in musculoskeletal system. In: Baert AL, Caramella D, Bartolozzi C (eds) 3D image processing: techniques and clinical applications. Springer, Berlin, pp 247–255

Damilakis J, Adams JE, Guglielmi G, Link TM (2010) Radiation exposure in X-ray-based imaging techniques used in osteoporosis. Eur Radiol 20:2707–2714

Dougeni E, Faulkner K, Panayiotakis G (2011) A review of patient dose and optimization methods in adult and paediatric CT scanning. Eur J Radiol [Epub ahead of print]

European Commission (1999) European guidelines on quality criteria for computed tomography. Report EUR 16262, Luxembourg

European Community (1997) Council directive 97/43/EURATOM, 30 June 1997, on health protection of individuals against the dangers of ionizing radiation in relation to medical exposure (repealing directive 84/466/Euratom). Off J Eur Commun L180 40:22–27

Fayad LM, Bluemke DA, Fishman EK (2005) Musculoskeletal imaging with computed tomography and magnetic resonance imaging: when is computed tomography the study of choice? Curr Probl Diagn Radiol 34:220–237

Foumani M, Strackee SD, Jonges R, Blankevoort L, Zwinderman AH, Carelsen B, Streekstra GJ (2009) In vivo three-dimensional carpal bone kinematics during flexion-extension and radio-ulnar deviation of the wrist: dynamic motion versus step-wise static wrist positions. J Biomech 42:2664–2671

Fuji K, Aoyama T, Yamauchi-Kawaura C, Koyama S, Yamauchi M, Akahane K, Nishizawa K (2009) Radiation dose evaluation in 64-slice CT examinations with adult and paediatric anthropomorphic phantoms. Br J Radiol 82: 1010–1018

Galanski M, Nagel HD, Stamm G (2001) CT radiation exposure risk in Germany. Rofo 173:R1–R66

Gervaise A, Louis M, Batch T, Loeuille D, Noel A, Guillemin F, Blum A (2010) Réduction de dose dans l'exploration du rachis lombaire grâce au scanner 320-détecteurs: étude initiale. J Radiol 91:779–785

Gervaise A, Osemont B, Lecocq S, Micard E, Noel A, Felblinger J, Blum A (2011) CT image quality improvement using adaptive iterative dose reduction with wide-volume acquisition on 320-detector CT. Eur Radiol [Epub ahead of print]

Gleeson TG, Morirty J, Shortt CP, Gleeson JP, Fitzpatrick P, Byrne B, McHugh J, O'Connell M, O'Gorman P, Eustace SJ (2009) Accuracy of whole-body low-dose multidetector CT (WBLDCT) versus skeletal survey in the detection of myelomatous lesions, and correlation of disease distribution with whole-body MRI (WBMRI). Skelet Radiol 38: 225–236

Goh V, Padhani AR (2006) Imaging tumor angiogenesis: functional assessment using MDCT or MRI? Abdom Imaging 31:194–199

Gurung J, Khan MF, Maataoui A, Herzog C, Bux R, Ackermann H, Vogl TJ (2005) Multislice CT of the pelvis: dose reduction with regard to image quality using 16-row CT. Eur Radiol 15:1898–1905

Hara AK, Paden RG, Silva AC, Kujak JL, Lawder HJ, Pavlicek W (2009) Iterative reconstruction technique for reducing body radiation dose at CT: feasibility study. Am J Roentgenol 193:764–771

Heck O, Louis M, Wassel J, Lecocq S, Gondim-Teixeira P, Moisei A, Blum A (2010) Apport du scanner volumique dynamique dans le diagnostic d'ostéome ostéoïde. Journées Françaises de Radiologie, Paris

Hidajat N, Wolf M, Nunnemann A, Liersch P, Gebauer B, Teichgraber U, Schroder RJ, Felix R (2001) Survey of conventional and spiral CT doses. Radiology 218:395–401

Horger M, Claussen CD, Bross-Bach U, Vonthein R, Trabold T, Heuschmid M, Pfannenberg C (2005) Whole-body lowdose multidetector row-CT in the diagnosis of multiple myeloma: an alternative to conventional radiography. Eur J Radiol 54:289–297

Hristova L, Batch T, Blum A (2009) Analyse des artéfacts de mouvement de l'exploration dynamique et volumique au scanner 320 barettes (abstract). J Radiol 90(10):1583

International Commission on Radiological Protection (1977) Recommendations of the International Commission on Radiological Protection, ICRP publication 26. Pergamon, Oxford

International Commission on Radiological Protection (1991) Recommendations of the International Commission on Radiological Protection. ICRP Publication 60. Pergamon, Oxford

Iochum S, Ludig T, Walter F, Fuchs A, Henrot P, Blum A (2001) Value of volume rendering in musculo-skeletal disorders. J Radiol 82:221–230

Jaffe TA, Yoshizumi TT, Toncheva G, Anderson-Evans C, Lowry C, Miller CM, Nelson RC, Ravin CE (2009) Radiation dose for body CT protocols: variability of scanners at one institution. Am J Roentgenol 193:1141–1147

Kalender WA, Deak P, Kellermeier M, van Straten M, Vollmar SV (2009) Application and patient size-dependent optimization of X-ray spectra for CT. Med Phys 36: 993–1007

Kalra MK, Maher MM, Toth TL, Hamberg LM, Blake MA, Shepard JA, Saini S (2004) Strategies for CT radiation dose optimization. Radiology 230:619–628

Kalra MK, Toth TL (2007) Patient centering in MDCT: dose effects. In: Tack D, Genevois PA (eds) Radiation dose from adult and pediatric multidetector computed tomography. Springer, Berlin, pp 129–132

Karcaaltincaba M, Aktas A (2011) Dual-energy CT revisited with multidetector CT: review of principles and clinical applications. Diagn Interv Radiol 17:181–194

Ketelsen D, Horger M, Buchgeister M, Fenchel M, Thomas C, Boehringer N, Schulze M, Tsiflikas I, Claussen CD, Heuschmid M (2010) Estimation of radiation exposure of 128-slice 4D-perfusion CT for the assessment of tumor vascularity. Korean J Radiol 11:547–552

Kröpil P, Fenk R, Fritz LB, Blondin D, Kobbe G, Mödder U, Cohnen M (2008) Comparison of whole-body 64-slice multidetector computed tomography and conventional radiography in staging of multiple myeloma. Eur Radiol 18:51–58

Lee TY, Chhem RK (2010) Impact of new technologies on dose reduction in CT. Eur J Radiol 76:28–35

Levine E, Neff JR (1983) Dynamic computed tomography scanning of benign bone lesions: preliminary results. Skelet Radiol 9:238–245

Li J, Udayasankar UK, Toth TL, Seamans J, Small WC, Kalra MK (2007) Automatic patient centering for MDCT: effect on radiation dose. Am J Roentgenol 188:547–552

Liu PT, Chivers FS, Roberts CC, Schultz CJ, Beauchamp CP (2003) Imaging of osteoid osteoma with dynamic gadolinium-enhanced MR imaging. Radiology 227:691–700

McNitt-Gray MF (2002) AAPM/RSNA physics tutorial for residents: topics in CT radiation dose in CT. Radiographics 22:1541–1553

Mahesh M (2009) Scan parameters and image quality in MDCT. In: Mahesh M (ed) MDCT physics: The basics—technology, image quality and radiation dose. Lippincott Williams & Wilkins, Philadelphia, pp 47–78

Mastora I, Rémy-Jardin M, Seuss C, Scherf C, Guillot JP, Rémy J (2001) Dose reduction in spiral CT angiography of thoracic outlet syndrome by anatomically adapted tube current modulation. Eur Radiol 11:590–596

McCollough CH, Bruesewitz MR, Kofler JM (2006) CT dose reduction and dose management tools: overview of available options. Radiographics 26:503–512

McCollough CH, Primak AN, Braun N, Kofler J, Yu L, Christner J (2009) Strategies for reducing radiation dose in CT. Radiol Clin North Am 47:27–40

Memarsadeghi M, Breitenseher M, Schaefer-Prokop C, Weber M, Aldrian S, Gäbler C, Prokop M (2006) Occult scaphoid fractures: CT versus MR imaging. Radiology 240: 169–176

Mettler FA, Huda W, Yoshizumi TT, Mahesh M (2008) Effective doses in radiology and diagnostic nuclear medicine: a catalog. Radiology 248:254–263

Miles KA, Charnsangavej C, Lee F, Fishman E, Horton K, Lee TY (2001) Application of CT in the investigation of angiogenesis in oncology. Acad Radiol 7:840–850

Moojen TM, Snel JG, Ritt MJ, Venema HW, Kauer JM, Bos KE (2003) In vivo analysis of carpal kinematics and comparative review of the literature. J Hand Surg Am 28: 81–87

Mori S, Endo M, Nishizawa K, Murase K, Fujiwara H, Tanada S (2006) Comparison of patient doses in 256-slice CT and 16-slice CT scanners. Br J Radiol 79:56–61

Mori S, Nishizawa K, Kondo C, Ohno M, Akahane K, Endo M (2008) Effective doses in subjects undergoing computed tomography cardiac imaging with the 256-multislice CT scanner. Eur J Radiol 65:442–448

Moser T, Dosch JC, Moussaoui A, Dietemann JL (2007) Wrist ligament tears: evaluation of MRI and combined MDCT and MR arthrography. Am J Roentgenol 188:1278–1286

Mulkens TH, Bellinck P, Baeyaert M, Ghysen D, Van Dijck X, Mussen E, Venstermans C, Termote JL (2005) Use of an automatic exposure control mechanism for dose optimization in multi-detector row CT examinations: clinical evaluation. Radiology 237:213–223

Mulkens TH, Marchal P, Daineffe S, Salgado R, Bellinck P, te Rijdt B, Kegelaers B, Termote JL (2007) Comparison of low-dose with standard-dose multidetector CT in cervical spine trauma. Am J Neuroradiol 28:1444–1450

Nagel HD (2007) CT parameters that influence the radiation dose. In: Tack D, Genevois PA (eds) Radiation dose from adult and pediatric multidetector computed tomography. Springer, Berlin, pp 51–79

Nakaura T, Awai K, Oda S, Yanaga Y, Namimoto T, Harada K, Uemura S, Yamashita Y (2011) A low-kilovolt (peak) high tube current technique improves venous enhancement and reduces the radiation dose at indirect multidetector-row CT venography: initial experience. J Comput Assist Tomogr 35:141–147

Nicolaou S, Yong-Hing CJ, Galea-Soler S, Hou DJ, Louis L, Munk P (2010) Dual-energy CT as a potential new diagnostic tool in the management of gout in the acute setting. Am J Roentgenol 194:1072–1078

Noel A, Ottenin MA, Germain C, Soler M, Villani N, Grosprêtre O, Blum A (2011) Comparison of irradiation for tomosynthesis and CT of the wrist. J Radiol 92:32–39

Oikarinen H, Meriläinen S, Pääkkö E, Karttunen A, Nieminen MT, Tervonen O (2009) Unjustified CT examinations in young patients. Eur Radiol 19:1161–1165

Oldrini G, Lombard V, Roch D, Detreille R, Lecocq S, Louis M, Wassel J, Batch T, Blum A (2009) Courbes de rehaussement des tumeurs osseuses et des parties molles: comparaison entre scanner et IRM (abstract). J Radiol 90:1578

Omoumi P, Mercier GA, Lecouvet F, Simoni P, Vande Berg BC (2009) CT arthrography, MR arthrography, PET, and scintigraphy in osteoarthritis. Radiol Clin North Am 47: 595–615

Pache G, Krauss B, Strohm P, Saueressig U, Blanke P, Bulla S, Schäfer O, Helwig P, Kotter E, Langer M, Baumann T (2010) Dual-energy CT virtual noncalcium technique: detecting posttraumatic bone marrow lesions- feasibility study. Radiology 256:617–624

Pantos I, Thalassinou S, Argentos S, Kelekis NL, Panayiotakis G, Efstathopoulos EP (2011) Adult patient radiation doses from non-cardiac CT examinations: a review of published results. Br J Radiol 84:293–303

Perisinakis K, Papadakis AE, Damilakis J (2009) The effect of X-ray beam quality and geometry on radiation utilization efficiency in multidetector CT imaging. Med Phys 36:1258–1266

Rehani MM, Bongartz G, Kalender W et al (2000) Managing X-ray dose in computed tomography: ICRP special task force report. Ann ICRP 30:7–45

Richards PJ, George J, Metelko M, Brown M (2010) Spine computed tomography doses and cancer induction. Spine 35:430–433

Schilham A, van der Molen AJ, Prokop M, Jong HW (2010) Overranging at multi-section CT: an underestimated source of excess radiation exposure. Radiographics 30: 1057–1067

Semelka RC, Armao DM, Elias J, Huda W (2007) Imaging strategies to reduce the risk of radiation in CT studies, including selective substitution with MRI. JMRI 25:900–909

Short WH, Werner FW, Fortino MD, Mann KA (1997) Analysis of the kinematics of the scaphoid and lunate in the intact wrist joint. Hand Clin 13:93–108

Shrimpton PC, Edyvean S (1998) CT scanner dosimetry. Br J Radiol 71:1–3

Silva A, Lawder H, Hara A, Kujak J, Pavlicek W (2009) Innovations in CT dose reduction strategy: application of the adaptive statistical iterative reconstruction algorithm. Am J Roentgenol 194:191–199

Singh S, Kalra MK, Thrall JH, Mahesh M (2011) CT radiation dose reduction by modifying primary factors. J Am Coll Radiol 8:369–372

Snel JG, Venema HW, Moojen TM, Ritt JP, Grimbergen CA, den Heeten GJ (2000) Quantitative in vivo analysis of the kinematics of carpal bones from three-dimensional CT images using a deformable surface model and a three-dimensional matching technique. Med Phys 27:2037–2047

Stierstorfer K, Kuhn U, Wolf H, Petersilka M, Suess C, Flohr T (2007) Principle and performance of a dynamic collimation technique for spiral CT (abstract). In: Radiological society of North America scientific assembly and annual meeting

program. Radiological Society of North America, Oak Brook, SSA16-04

Stradiotti P, Curti A, Castellazzi G, Zerbi A (2009) Metal-related artifacts in instrumented spine: techniques for reducing artifacts in CT and MRI: state of the art. Eur Spine J 18:S102–S108

Subhas N, Freire M, Primak AN, Polster JM, Recht MP, Davros WJ, Winalski CS (2010) CT arthrography: in vitro evaluation of single and dual energy for optimization of technique. Skelet Radiol 39:1025–1031

Tay SC, Pimak AN, Fletcher JG, Schmidt B, Amrami KK, Berger RA, Mc Collough CH (2007) Four-dimensional computed tomographic imaging in the wrist: proof of feasibility in a cadaveric model. Skelet Radiol 36: 1163–1169

Thévenin FS, Drapé JL, Biau D, Campagna R, Richarme D, Guerini H, Chevrot A, Larousserie F, Babinet A, Anract P, Feydy A (2010) Assessment of vascular invasion by bone and soft tissue tumors of the limbs: usefulness of MDCT angiography. Eur Radiol 20:1524–1531

Thomton FJ, Paulson EK, Yoshizumi TT, Frush DP, Nelson RC (2003) Single versus multi-detector row CT: comparison of radiation doses and dose profiles. Acad Radiol 10:379–385

Tins BJ, Cassar-Pullicino VN, Lalam RK (2007) Magnetic resonance imaging of spinal infection. Top Magn Reson Imaging 18(3):213–222

van der Molen AJ, Geleijns J (2007) Overranging in multisection CT: quantification and relative contribution to dose—comparison of four 16-section CT scanners. Radiology 242:208–216

van Straten M, Deak P, Shrimpton PC, Kalender WA (2009) The effect of angular and longitudinal tube current modulations on the estimation of organ and effective doses in X-ray computed tomography. Med Phys 36(11):4881–4889

von Falck C, Galanski M, Shin H (2010) Sliding-thin-slab averaging for improved depiction of low-contrast lesions with radiation dose savings at thin-section CT. Radiographics 30:317–326

Wallace AB, Goergen SK, Schick D, Soblusky T, Jolley D (2010) Multidetector CT dose: clincal pratice improvement strategies from a successful optimization program. J Am Coll Radiol 7:614–624

West ATH, Marshall TJ, Bearcroft PW (2009) CT of the musculoskeletal system: what is left is the days of MRI? Eur Radiol 19:152–164

Wolfe SW, Neu C, Crisco JJ (2000) In vivo scaphoid, lunate and capitate kinematics in flexion and in extension. J Hand Surg Am 25:860–869

Wyler A, Bousson V, Bergot C, Polivka M, Leveque E, Vicaut E, Laredo JD (2009) Comparison of MR-arthrography and CT-arthrography in hyaline cartilage-thickness measurement in radiographically normal cadaver hips with anatomy as gold standard. Osteoarthr Cartil 17:19–25